International Journal of Technical Research and Applications e-ISSN: 2320-8163,
www.ijtra.com Special Issue 38 (February, 2016), PP. 73-78

DIELECTRIC AND MECHANICAL STUDIES ON PURE AND MG^{2+} DOPED ZTS SINGLE CRYSTAL

M. Sumithra Devi[1,2], A.P. Arthi [3], K. Thamizharasan[*]

[1]Department of Physics, AIHT, Chennai-603 103 Tamilnadu
[2]Research Scholar, R&D center, Coimbatore, Tamilnadu
[3]Department of Physics, Thangavelu Engineering College -600097 Chennai, Tamilnadu
[*]Department of Physics, Sir Theagaraya College, Chennai - 600021, Tamilnadu

Abstract: **Pure and Mg^{2+} doped ZTS, a semiorganic single crystal has been grown by slow evaporation solution growth technique at room temperature. The growth of pure and Mg^{2+} doped ZTS were confirmed by single crystal X-ray diffraction analysis. Result of indentation – induced hardness testing is presented. The Vicker's Micro hardness of the material in the load range 25 - 200g were pure (111.89 – 210.732) and Mg^{2+} doped ZTS (96.52 – 172. 92) Kg/mm^2. The values of elastic stiffness constant, fracture mechanics, brittleness index and yield strength have also been calculated. The dielectric measurements of the crystal in the frequency range 1 KHz – 1MHz were investigated. The activation energy of electrical process was also calculated and reported.**

Keyword: **Solution growth, Microhardness, Dielectric studies.**

1. Introduction

Thiourea molecule is known to possess a large dipole moment and also has the ability to form a network of hydrogen bonds. Thiourea molecule can coordinate with numerous metal ions to form stable coordination complexes [1]. Nonlinear optics plays an important role in the emerging photonic and optoelectronic technologies. Nonlinear optical (NLO) materials find wide application, data storage technology and the electro –optic modulation [2-7]. In addition to large second order susceptibilities, good transmission in UV visible region and stable physico thermal performance are needed for these applications[8-9]. ZTS is one of the excellent and efficient NLO materials among the thiourea complexes. ZTS crystals also possess good mechanical properties and their second harmonic conversion is high compared to KDP crystals [10]. Since the data on mechanical properties and dielectric properties of slow evaporation solution growth of pure and Mg^{2+} doped for the first time we present our investigations.

2. Experimental

2.1. Growth technique

The AR grade of ZTS salt was synthesized by dissolving zinc sulphate and thiourea with the molar ratio 3:1 in Millipore water. The solution was stirred using magnetic stirrer. A saturated solution was prepared using the recrystallized salt and de-ionized water at room temperature with continuous stirring. The growth of Mg^{2+} doped ZTS crystals 1 mol % of magnesium sulphate was added to the saturated solution of ZTS and stirred continuously to ensure homogeneous concentration. The solution was filtered and kept undisturbed at room temperature for slow evaporation technique. Optically good quality seed crystals were grown from the solution. To improve transparency recrystalization was done many times. Transpearent Mg^{2+} doped ZTS crystals with well defined morphology were obtained by spontaneous crystallization. Mg^{2+} crystals of size (9X5X6 mm^3) were obtained in the growth period of 25 days. The grown of pure and Mg^{2+} doped ZTS crystal was shown in Figure 1.

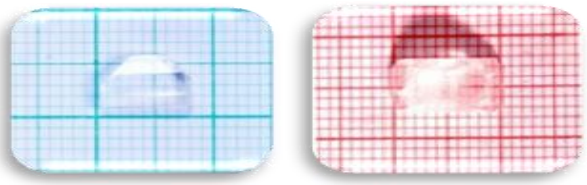

Figure1. Photograph of as grown pure and Mg^{2+} doped ZTS crystals

2.2. Microhardness tests

In the view of device fabrication, calculation of localized plastic deformation is very important [11]. This can be done with the help of Vicker's Micro hardness studies. In this present investigation smooth surface of the crystal was chosen and the diamond indenter was allowed to indent on the surface for 10 seconds. The applied load was varied from 25 – 200gm. The indentation was done on different places of the crystal surface. Hardness value was calculated from the relation[12].

$$H_v = 1.8544 \times \frac{p}{d^2} \text{ Kg/mm}^2 \quad (1)$$

Where P was taken in Kg and was in μm.

The fracture toughness of the material was given by the relation[13]

$$K_c = \frac{P}{\beta_0 (C)^{3/2}} \quad (2)$$

Where P is applied load in Kg, C is the crack length measured and β_0 is taken as 7 for Vicker's indenter. The above equation holds good only for the cracks due to an elastic stress field formed during the time of indentation [14-16]. The fracture induced brittle ness is an important property which affects the mechanical behavior of the material and it was calculated by the relation [17,18].

$$B_i = \frac{H_v}{K_c} \quad (3)$$

The yield strength of the material can be calculated from the hardness value [19]. If Mayer's index n>2

$$\sigma_v = \frac{H_v}{2.9}\left[1-(2-n)\right]\left[\frac{12.5(2-n)}{1-(2-n)}\right]^{2-n} \quad (4)$$

Elastic stiffness constant (C_{11}) can be calculated using the relation [20]

$$C_{11} = (H_v)^{\frac{7}{4}} \quad (5)$$

2.3 Dielectric measurements

The main dielectric parameters are dielectric constant (ε_r), dielectric loss (tan δ), ac conductivity (σ_{ac}), dc conductivity (σ_{dc}) and Modulus (M' and M''). These properties give the distribution of electric field within the solid [21]. Study of dielectric property of the material is very important as it provides an insight into the polarization process that takes place in the material[22]. The behavior of the charge carriers under an electric field, their mobility and mechanism of conduction provide information about the usefulness of the materials for different applications[23]. In the present investigation, the dielectric measurement of the crystals were carried out by the parallel plate capacitor method for different temperatures and frequencies[18] using HIOKI 3532 – 50 LCR HITESTER. The dielectric constant ε_r can be defined as the ratio of the electric field density produced in the medium to that produced in vacuum (air medium) by the same dielectric field strength. Therefore the relative dielectric constant ε_r is

$$\varepsilon_r = \frac{\varepsilon}{\varepsilon_0} \quad (6)$$

Where ε_0 is called the absolute permittivity and is equal to $8.854X10^{-12}$ farad/meter. Where **ε**

$$\varepsilon = \frac{cd}{A} \quad (7)$$

then ε_r became

$$\varepsilon_r = \frac{Cd}{\varepsilon_0 A} \quad (8)$$

where A is the area of the sample and d is the thickness of the sample. The relative permittivity (**ε_r**) is usually known as permittivity. It is always greater than unity. The dielectric loss is defined as the loss of power under the action of voltage. The loss was due to the conversion of moment of charges into vibration of lattice the crystal. When an electric field is applied to a dielectric material the charge stored in the material real and imaginary component[25] (in-phase and out - of – phase). Thus dielectric property is a complex quantity and it is given by,

$$\varepsilon = \varepsilon' - i\varepsilon'' \quad (9)$$

where **ε** is dielectric permittivity, **ε′** is real part of dielectric permittivity and **ε′′** is imaginary part of dielectric permittivity.

The dielectric loss factor (tan δ), which is measure of the electric energy dissipated in to thermal energy was defined by,

$$\text{Tan } \delta = \frac{\varepsilon''}{\varepsilon'} \quad (10)$$

Knowing the values of dielectric constant (ε_r) and the loss factor (tan δ), the ac conductivity was estimated using the relation,

$$\sigma_{ac} = 2\pi f \varepsilon_0 \varepsilon_r \tan \delta \quad (11)$$

where f is the frequency of the applied field.

All the dielectric parameters (dielectric constant, loss tangent and ac conductivity) depends on the external factors such as frequency of the applied field, pressure, humidity etc[26,27]. The activation energy of the material is calculated using the Arrenius plot of In σ using the relation [28].

$$\sigma_{ac} = \sigma_0 e^{\left[\frac{-E}{KT}\right]} \quad (12)$$

where σ_0 is the pre-exponential factor, K is Boltzman constant, E is activation energy, and T is the absolute temperature.

2.4 Result and Discussion

2.4.1 X-ray diffraction single crystal analysis

Single crystal XRD analysis has been carried out to estimate the lattice parameters, the arrangement and the spacing of atoms in the crystalline material. The data has been collected using Enraf Nonius CAD-4 single crystal X-ray diffractrometer with MoKα (λ = 0.71073 Å) radiation. It were observed from the single crystal XRD data that the grown both crystals of pure and Mg^{2+} doped ZTS possesses orthorhombic crystal system with space group $Pca2_1$. The lattice parameters of pure ZTS is a = 7.78 Å, b = 11.124 Å and c = 15.491 Å, α=β=γ=90° and Mg^{2+} doped ZTS is a =7.78 Å, b = 11.164 Å and c = 15.531 Å, Å, α=β=γ=90°. The volume of the crystal were pure 1341 $Å^3$ and Mg^{2+} doped ZTS 1348 $Å^3$. The single crystal XRD data confirmed that the as grown crystal were pure and Mg^{2+} doped ZTS [29-31].

2.4.2 Microhardness Analysis

Figure 2 shows the variation of Vicker's hardness number against applied load for pure and Mg^{2+} doped ZTS crystal. The plot indicated that the harness number of the crystal increased with increase in load. A steep rise in hardness number was observed in the range 25 – 200gm and have maximum H_v at about 200gm which showed Reverse Indentation Size Effect(RISE). The load variation can be interpreted by using mayer's law $P=a.d^n$ [32]. Mayer's index (n) has been calculated from plot of log P vs log d in Figure 3 which yielded a straight line and its slope value gave the work hardening coefficient (or) Mayer's index 'n' which was found to be pure (2.83) and Mg^{2+} doped ZTS (2.85). According to Onitsch n should lies between 1 and 1.6 for hard materials and it should be more than 1.6 for soft materials[33]. Hence, it is concluded that both crystals are soft in nature.The Yield strength of the material (σ_v), Elastic stiffness constant (C_{11}), Fracture mechanics (K_c), and Brittleness index (B_i) were calculated from hardness value and presented in Table 1 and 2 for pure and Mg^{2+} doped ZTS single crystal.

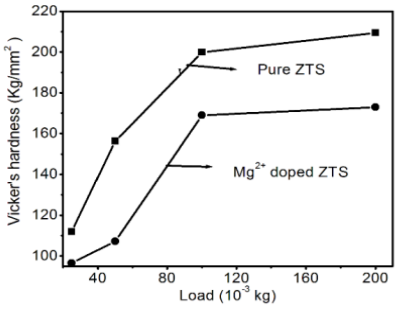

Fig 2. Variation of Vicker's hardness with load of pure and Mg^{2+} doped ZTS single crystal

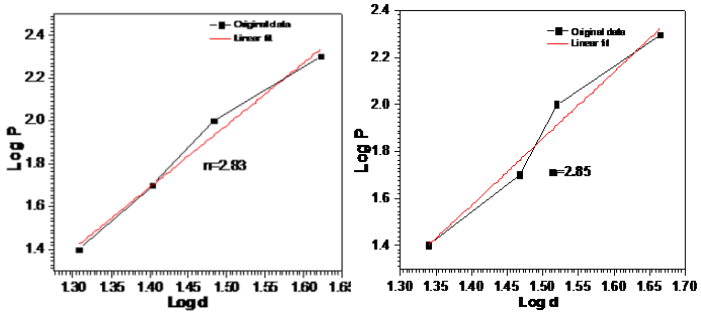

Fig3. Variation of log P with log d of pure and Mg^{2+} doped ZTS single crystal

Table 1 Michrohardness Parameters of pure ZTS crystal

Load X10^{-3}Kg	H_v Kg/mm^2	C_{11}	K_c (Kg/mm$^{3/2}$)	B_i (mm$^{-1/2}$)	σ_v Kg/mm^2
25	111.89	3849	0.10999	10.172	200.63

50	156.284	6970	0.16805	9.299	280.24
100	199.08	10551	0.24038	8.282	356.98
200	210.732	11655	0.29739	7.086	377.88

Table 2 Michrohardness Parameters of Mg^{2+} doped ZTS crystal

Load X10^{-3}Kg	H_v Kg/mm^2	C_{11}	K_c (Kg/mm$^{3/2}$)	B_i (mm$^{-1/2}$)	σ_v Kg/mm^2
25	96.5	2972.2	0.09853	9.7959	186.64
50	107.2	3572.3	0.12669	8.4631	207.33
100	168.9	7917.0	0.21187	7.9742	326.69
200	172.9	8245.5	0.25641	6.7439	334.37

2.4.3 Dielectric Characteristics

The dielectric studies on pure and Mg^{2+} doped ZTS single crystal was carried on its most prominent face. A sample of dimension of pure (4x3x3) and Mg^{2+} doped ZTS (4x3x2) mm^3 having silver coating on the opposite faces was placed between two copper electrodes and thus a parallel plate capacitor was ranged 313 K to 423 K.

The dependence of dielectric constant with frequency of pure and Mg^{2+} doped ZTS crystals were showed in Figure 4. At low temperatures (313K) and at high temperatures (423K) real dielectric constant decreased in the frequency range 1 KHz to 1MHz. The rate of decrease in dielectric constant was higher at higher temperature and lower at lower temperature ranges.

Figure 5 showed the imaginary dielectric constant (ε'') versus frequency plots at various temperatures of pure and Mg^{2+} doped ZTS. The dependence of imaginary dielectric constant was similar to that of the real part of dielectric constant in the temperatures range 313 K to 423 K. At low temperatures (313 K) and higher temperatures (423 K) dielectric constant decreased. Rate of decrease in imaginary dielectric constant was higher at higher temperatures and lower at lower temperatures and it decreased when the frequency increased [34]. This type of dependence of ε'' was similar for all frequency ranges.

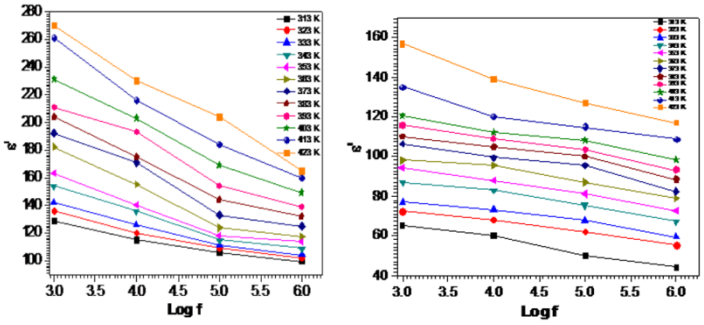

Fig 4. Plot of log f with ε' of pure and Mg^{2+} doped ZTS single crystal

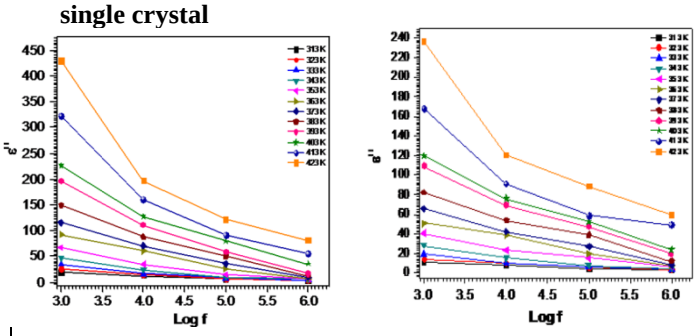

Fig 5. Plot of log f with ε'' of pure and Mg^{2+} doped ZTS single crystal

Figures 6 showed that the loss tanget versus frequency plots at various temperatures for pure ZTS and Mg^{2+} doped ZTS. At low temperatures (313K) and higher temperatures (423K) dielectric loss decreased as the field was increased from 1 KHz to 1 MHz. The fall in dielectric loss were greater as the temperature increased from 313K to 423K and decreased with increase in frequency in all temperatures.

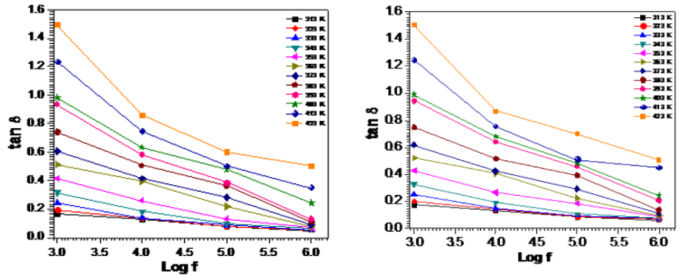

Fig 6. Plot of log f Vs. tanδ of pure and Mg^{2+} doped ZTS single crystal

Crystal with high dielectric constant leads to power dissipation. The material having low dielectric constant has less number of dipoles per unit volume. As a result, they have maximum loss as compared to the material having a high dielectric constant[35]. According to our experiment observations the values of real, imaginary dielectric constant increased with temperature at all frequencies which lead to the conclusion from space polarization, α_s with temperature. At the same time dielectric constant decreased with increase in frequency for all temperature range. Therefore, low dielectric constant of growing crystal at higher frequency was an added advantage for high speed electro optic modulation device fabrication.

The dependence of ac conductivity on the temperature at different frequencies (1 KHz, 10 KHz, 100 KHz and 1 MHz) were shown in Figure 7 for pure and Mg^{2+} doped ZTS single crystal. The value of ln (σac) increased in the lower (1KHz) and higher frequencies (1MHz). A similar variation were observed at other frequencies like 10 KHz and 100 KHz. The value conductivity were found to decrease with increase in frequency.

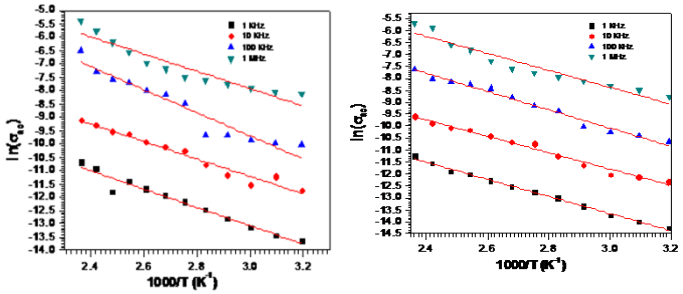

Fig 7.Arrhenius plot of pure and Mg^{2+} doped ZTS single crystal

The activation energy for various frequencies were calculated from slope of the graph between ln (σac) and 1000/T and were found to be very linear as showed in Figures 7 for pure and Mg^{2+} doped ZTS single crystal. Figure 8 showed that the variation of activation energy with log f. From the graph, it were found that the activation energy decreased with increase in frequency.

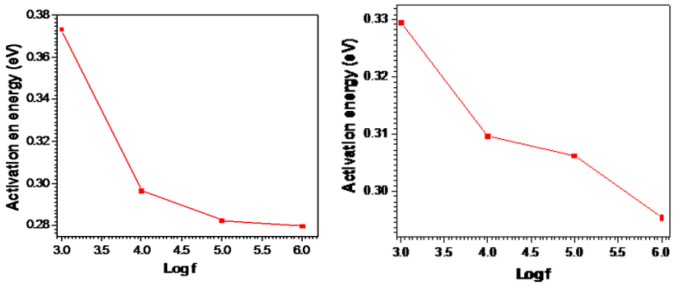

Fig 8. Plot of log f Vs. activation energy of pure and Mg^{2+} doped ZTS single crystal

Acknowledgement

The authors acknowledge SAIF, IIT-Madras, Loyola college, India for characterization facilities.

Conclusion

A semi-organic crystal, pure and Mg^{2+} doped ZTS were grown successfully by slow evaporation solution growth technique. Single crystal X-ray diffraction study that the grown crystal belongs to orthorhombic crystal system. Vicker's microhardness measurements reveals that both crystals are soft in nature and shows reverse indentation size effect. Various mechanical parameters were calculated and tabulated. Dielectric properties of the as grown crystal were analyzed by measuring dielectric loss and capacitance of the material in different frequencies in different temperatures. The dielectric loss and dielectric constant increased when we increase the frequency in all temperatures. At lower frequencies all four polarizations were present and when the frequency was increased only electronic polarization was present. To fine the ac conductivity of the material a graph was drawn between temperature and $\ln\sigma_{ac}$. It was found from the graph that when the temperature was increased the conductivity of the material also increased in all temperatures. To find the activation energy, Arrhenius plot were drawn and it was found that the activation energy decreased when the frequency was increased.

References

[1] Sonia Bhandari , Nidhi Sinha , Geeta Ray , Binay Kumar, J. chemical Physics Letters. 591**(2014)**, 10 – 15.

[2]. Meera K, Muralidharan R, Dhanasekaran R, Manyum Prapun, Ramasamy P, J.Cryst.Growth.263 **(2004)**,510-516.

[3].Mohan Kumar R, Rajan Babu D, Jayaraman D, Jayavel R, Kitmura K, J.Cryst.Growth.275, **(2005)**, e1935-e1938.

[4] Pricilla Jeyakumari,Ramajothi J, Dhanuskodi S, J.Cryst. Growth.269 **(2004)**, 558-564.

[5] Haja Hameed A.S, Lan C.W, J.Cryst. Growth.270 **(2004)**, 475-480.

[6] Hussaini S.S, Dhumane N.R, Dongre V.G, Shirsat M.D, J.Materials Science-Poland 27 (2009), 365-372.

[7] Shaokang Gao', Weijun Chen', Guimei Wang', Jianzhong Chen, J.Cryst. Growth. 297 **(2006)**, 361-365.

[8] Joseph Ginson P, Philip J, Rajarajan K, Rajasekar S.A, Joseph Arul Pragasam A, Thamizharasan K, Ravi Kumar S.M, Sagayaraj P, J.Cryst.Growth. 296 **(2006)**, 51-57.

[9] Ushasree P.M, Muralidharan R, Jayavel R, Ramasamy P, J.Cryst.Growth. 210 **(2000)**,741-745.

[10] Ushasree P.M, Jayavel R, Subramanian C, Ramasamy P, J. Cryst. Growth 197, **(1999)**,216.

[11] Westbrook J.H, Conerd H, American Society for Metals, Ohio, Cambridge University Press, Cambridge, **1971**.

[12] Mott B.W, Microindentation hardness Testing, Butterworths, London, **1966**,pp.9.

[13] Lawn B.R, E.R.Fuller, J.Matter.Sci.10 **(1975),** 2016.

[14] Ishikaa H, Skinkai N, J.Am.Ceram.Soc.65 **(1980)** C-124.

[15] Lawn B.R, Evans A.G, J.Mater.Sci. 12 **(1977)** 2195.

[16] Lawn B.R, Evans A.G, Marshall D.B, J.Am.Ceram. Soc. 63 **(1980)** 574.

[17] Nihara K, Morena R, Hasselman D.P.H, J.Matter. Sci. Lett. 1 **(1982)** 13.

[18] Singh I.V, Mishra B.K, Sachin Kumar, Shedbale A.S, International Journal of advanced Materials manufacturing and characterization, 4 **(2014)** 11.

[19] Cahoon J.P, Broughton W.H, Katzuk A.R, Metall. Trans. 2 **(1971)** 1979.
[20] Lawn B.R, Marshall D.B, J. Am. Ceram. Soc. 65 **(1979)** 347.
[21] David C. Jiles, Introduction to the electronic properties of Material -2nd Edition, CRC Press, London, **2010**.
[22] Tareev, Physics of Dielectric Materials, Mir Publisher, Moscow, **1979**.
[23] Xue D, Betzler K, Hesse H, Journal of Physics. Condensed Matter, 12 **(2000)** 3113.
[24] Perumal S, Mahadevan C.K, Physica B, 367 **(2005)** 172-181.
[25] Chilton J.A, Goossey M.T, Special Polymers for Electronics and Optoelectronics, Chapman and Hall, London, **1995**.
[26] Kasap S.O, Principles of electronic materials and devices, Tata McGrew Hill Education Pvt. Ltd, New Delhi, **2007.**
[27] Vasudevan A, Carin S, Mclloch M.R, 73 **(1978)** 671.
[28] Verwey E.J.W, Heilman E.L, J. Chem. Physics, 15 **(1947)** 174.
[29] Ushasree P.M, Jayavel R, Ramasamy P, Mater Sci. Engg. B 65 **(1999)**, 153-158.
[30] Ushasree P.M, Jayavel R, Ramasamy P , Mater. Chem. Phys. 61 **(1999)**, 270- 274.
[31] Arunmozhi G, M.de E.gomes, Ganesamoorthy S, Cryst. Res. Technol, 39 **(2004)**, 408-413.
[32] Sangwal K, Cryst. Res. Tech., 44**(2009)** 1019-1037.
[33] Onitsch E.M, Mikroskopie, 95 **(1956)** 12-14.
[34] Kambale R.C, Shaikh P.A, Bhosale C.H, Rajpur K.Y, Kolekar Y.D, Smart Materials and structures, 17 **(2009)** 115028.
[35] Dalton L.R, Journal of Physics, Condensed Matter, 15 **(2003)** 897.

.